

POLYMERS

High strength in combination with high toughness in robust and sustainable polymeric materials

Xiaojuan Liao¹, Martin Dulle², Juliana Martins de Souza e Silva³, Ralf B. Wehrspohn^{3,4}, Seema Agarwal¹, Stephan Förster^{2,5}, Haoqing Hou⁶, Paul Smith⁷, Andreas Greiner^{1*}

In materials science, there is an intrinsic conflict between high strength and high toughness, which can be resolved for different materials only through the use of innovative design principles. Advanced materials must be highly resistant to both deformation and fracture. We overcome this conflict in man-made polymer fibers and show multifibrillar polyacrylonitrile yarn with a toughness of 137 ± 21 joules per gram in combination with a tensile strength of 1236 ± 40 megapascals.

The nearly perfect uniaxial orientation of the fibrils, annealing under tension in the presence of linking molecules, is essential for the yarn's notable mechanical properties. This underlying principle can be used to create similar strong and tough fibers from other commodity polymers in the future and can be used in a variety of applications in areas such as biomedicine, satellite technology, textiles, aircrafts, and automobiles.

Synthetic materials with a combination of high strength and high toughness are rare and represent an important technological challenge (1). Engineered metal alloys (2), metallic glass composites (3), nanocellulose paper (4), glass (5), and carbon-based materials (6–9) are some examples of materials with this property combination. High resistance to both deformation (high strength) and fracture (high toughness) is achieved in man-made single-polymer nanofibers of very small diameter by electrospinning (10–14). However, these single nanofibers are not robust enough for handling for real-world applications. Natural fibers, like dragline spider silks (15, 16) and recombinant spider silks (17), achieve the

combination of high strength and high toughness as well, but their applicability is restricted by either low availability or high prices for various applications.

We discovered a straightforward concept for combination of high strength and high toughness through the preparation of polymeric fibers by yarn electrospinning, which creates fibers consisting of thousands of aligned nanofibrils in combination with a specified amount of a linker molecule. Simple alignment of the nanofibrils in electrospun yarns in combination with a high degree of crystallization does not result in high toughness in conjunction with high strength. Rather, this combination is achievable through the addition of a small

amount of an interconnecting molecule during yarn electrospinning and annealing after the heat stretching of the nanofibrils.

We fabricated the high-strength and high-toughness polymer yarns in three steps (fig. S1). First, continuous yarns were obtained by yarn electrospinning a solution of commercial polyacrylonitrile (PAN) {Dolan, copolymer with 4.18 mole % [6.35 weight % (wt %)] methyl acrylate according to our ¹H-NMR (proton nuclear magnetic resonance) analysis, number average molar mass (M_n) = 120,000; molar mass dispersity (D) = 2.79} and different amounts of the bifunctional poly(ethylene glycol) bisazide (PEG-BA) as an interconnecting molecule. Azides were applied in “click” reactions (18). These yarns were then stretched at 160°C in air. The stretched yarns were further annealed at 120°, 130°, and 140°C under tension for several hours, which finally resulted in high-strength and high-toughness yarns, depending on the applied conditions and the composition of PAN and PEG-BA (we tested amounts ranging from 0 to 6 wt % of

¹Macromolecular Chemistry and Bavarian Polymer Institute, University of Bayreuth, 95440 Bayreuth, Germany. ²JCNS-1/ICS-1, Forschungszentrum Jülich, 52425 Jülich, Germany.

³Institute of Physics, Martin Luther University Halle-Wittenberg, Heinrich-Damerow-Straße 4, 06120 Halle (Saale), Germany. ⁴Fraunhofer Institute for Microstructure of Materials and Systems (IMWS), Walter-Hülse-Straße 1, 06120 Halle (Saale), Germany. ⁵Physical Chemistry, Rheinisch-Westfälische Technische Hochschule Aachen University, 52074 Aachen, Germany. ⁶College of Chemistry and Chemical Engineering, Jiangxi Normal University, Nanchang, Jiangxi 330022, People's Republic of China. ⁷ETH Zürich, HCP F41.2, 8093 Zürich, Switzerland.

*Corresponding author. Email: greiner@uni-bayreuth.de

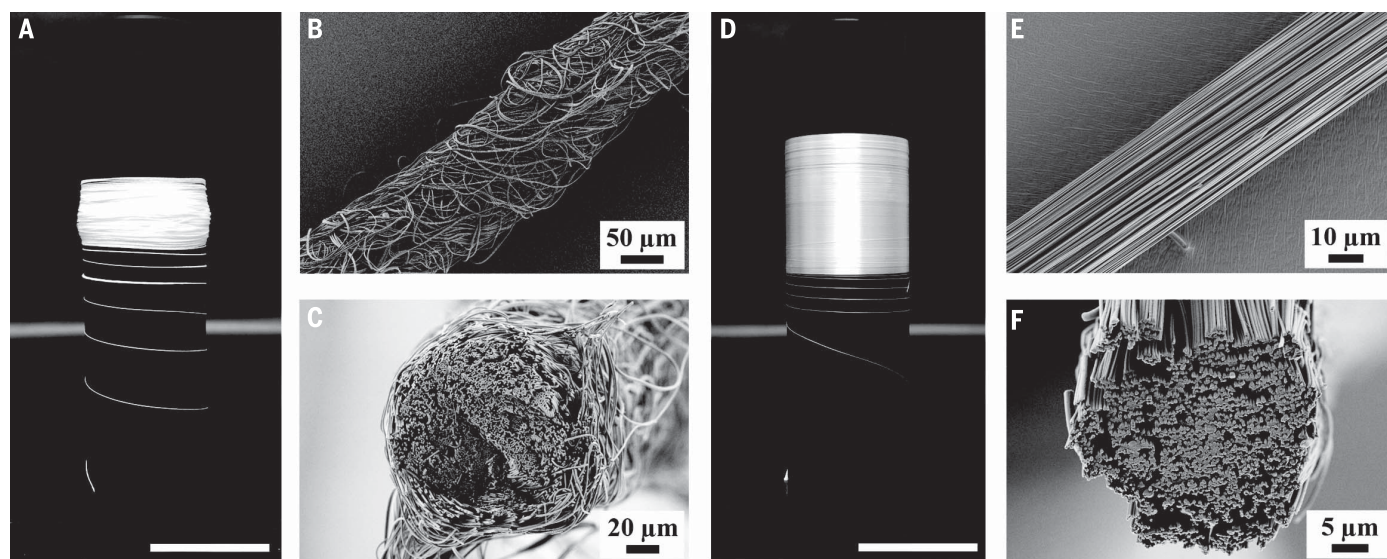


Fig. 1. Photographs and scanning electron microscopy (SEM) images of the yarns. (A) Photograph of continuous as-spun yarns. (B) SEM image of the long axis of the as-spun yarns. (C) SEM image of a cross-section of the as-spun yarns. (D) Photograph of stretched yarns. (E) SEM image of the long axis of stretched (at SR 8 at 160°C) and annealed (130°C for 4 hours) yarns (EASY). (F) SEM image of a cross-section of the stretched (at SR 8 at 160°C) and annealed (130°C for 4 hours) yarns (EASY). The scale bars in the photographs of the as-spun yarns (A) and stretched yarns (D) are 20 mm.

PEG-BA relative to PAN). The electrospun, stretched, and annealed yarns are hereafter abbreviated as EASYs; the yarns processed with PEG-BA are abbreviated as i-EASYs.

In a model study for the systematic understanding of the effect of stretching with commercial PAN without PEG-BA, we found that as-spun yarns had an average diameter of $130 \pm 12 \mu\text{m}$ and consisted of ~ 3000 nonoriented individual fibrils with $1.17 \pm 0.12 \mu\text{m}$ diameter (Fig. 1, A to C, and fig. S2, A and B). Heat stretching of the yarns for several minutes resulted in their manifold elongation accompanied by a change in the macroscopic appearance (Fig. 1D) and the alignment of the fibrils in the yarns (Fig. 1E). Stretching needed to be conducted above the glass transition temperature (T_g) of PAN ($T_g = 103^\circ\text{C}$ according to our differential scanning calorimetry measurement) but below the onset of oxidation at 180°C (19). We investigated yarns with different stretch ratios (SRs) ranging from 1 to 9 (where SR is the length of stretched yarn divided by the length of as-spun yarn, and a SR of 1 is unstretched) at stretch temperatures of 130° and 160°C and determined the alignment factor. The alignment factor [orientation of the fibrils of the yarn, with values ranging from 0 for an isotropic orientation to 100% for a perfect alignment (20)] increased from $\sim 46.0\%$ (at SR 1) to 99.6% at SR 9 and stretch temperature 160°C (fig. S3A). The orientation of the fibrils can also be seen in the three-dimensional (3D) x-ray images of the yarn samples (fig. S4 and movies S1 and S2). The tortuosity estimation, calculated using the 3D images, is equal to 1.00 for stretched yarns (at SR 8 at 160°C) and agrees well with the uniform orientation of the fibrils. The stretching of yarns naturally caused a reduction of their diameter, from $130 \pm 12 \mu\text{m}$ (unstretched yarns) to $50 \pm 3.3 \mu\text{m}$ (at SR 5 at 130°C) and $36 \pm 1.3 \mu\text{m}$ (at SR 9 at 160°C) (fig. S2, C and D). Simultaneously, the diameters of the fibrils reduced from $1.17 \pm 0.12 \mu\text{m}$ to $0.57 \pm 0.01 \mu\text{m}$ and to $0.37 \pm 0.07 \mu\text{m}$ at 130° and 160°C , respectively (Fig. 1F and fig. S3B). The reduction in diameter of the yarns after stretching can be explained by the untwisting and alignment of the fibrils. Stretching also reduced the linear densities of the yarns, which changed from $3.74 \pm 0.14 \text{ tex}$ [mass of fiber (g)/1000 m] in the as-spun yarns to $0.39 \pm 0.04 \text{ tex}$ at SR 9 at 160°C (fig. S3C). After heat stretching, annealing under tension (about 15 to 20 cN) was applied to achieve high toughness and high strength of the yarns. This annealing step (130°C for 4 hours in air) did not result in any further changes in the diameters of the yarns (EASY) or of the fibrils (fig. S3D).

The results of the model studies were transferred to yarns composed of PAN and the interconnecting molecule PEG-BA. Bisazides were reported to undergo the [2+3] click azide cyclo-

addition reaction (18) with the acrylonitrile groups of PAN, which could either favorably lead to bridging between the fibrils in the yarns or cause reaction with PAN in the bulk of the yarns. PEG-BA contents in yarns in the range from 0 to 4 wt % had no significant effect on the diameter of stretched and annealed yarns (fig. S3D). To analyze the effect of PEG-BA on the mechanical properties of the yarns, the toughness and the specific strength were analyzed for stretched yarns with different contents of PEG-BA relative to PAN. The maximum stress (fig. S5A) and modulus (fig. S5B) increased with the SR, whereas the toughness did not linearly increase with the SR (fig. S5C). The increase of PEG-BA content decreased the maximum stress and modulus slightly (fig. S5, D and E). In contrast, the toughness increased slightly (fig. S5F). However, the subsequent annealing step had a significant effect on the toughness of the yarns when PEG-BA was present. An annealing time of 4 hours was found to be optimal for the maximum strength, modulus, and toughness at an annealing temperature of 130°C (fig. S5, G to I). Optimum values were obtained with 4 wt % PEG-BA, at SR 8 at 160°C , with subsequent annealing at 130°C for 4 hours (Fig. 2 and Fig. 3, A and C). These yarns (i-EASY) have a tensile strength of $1236 \pm 40 \text{ MPa}$, a modulus of $13.5 \pm 1.1 \text{ GPa}$, and a toughness of $137 \pm 21 \text{ J/g}$, which are similar properties to those of dragline spider silk (15, 16). They also have a value for the tensile modulus of 13.5 GPa , which is close to the theoretical limit calculated for atactic crystalline PAN fibers (21). For comparison, the strength of an aligned, electrospun PAN nonwoven is $110 \pm$

12 MPa and its toughness is $57 \pm 3.0 \text{ J/g}$. Untreated as-electrospun PAN yarn has a strength of $72 \pm 3.0 \text{ MPa}$ and its toughness is $76 \pm 10 \text{ J/g}$. The linear density of i-EASY was only $0.4 \pm 0.06 \text{ tex}$ and it had an alignment factor of the fibrils of 99.4% . This yarn, weighing 0.008 mg , could lift a total mass of up to 30 g repeatedly without breaking (movie S3) and could even be used to sew a button to a shirt (movie S4). After repeatedly lifting 30-g weights, the yarn elongated slightly, most likely because of the elongation at the yielding point (strain of $\sim 2.5\%$). Even after 5000 cycles of loading and unloading at a maximum tensile strength of 400 MPa , only a negligible change in the final tensile strength ($\sim 5.3\%$) and plastic deformation ($\sim 4.2\%$) was observed (fig. S6, A and B). The plastic deformation occurred mainly in the first 10 cycles. Owing to minor structural changes after 10 cycles, the energy loss coefficient with cycling showed a slight decrease, with values in the range of 0.23 to 0.15 (fig. S6C).

On the basis of our findings, we postulate that only the combination of high-fibril orientation, caused by stretching and annealing in the presence of a certain amount of PEG-BA as an interlinking molecule, yielded high strength and high toughness in combination with high crystallinity (Fig. 3, A to C). Clearly, the crystallinity of the PAN in the yarns is insufficient on its own for the achievement of high strength in combination with high toughness. Polarized Raman spectroscopy confirmed that the heat stretching procedure caused the orientation of the PAN macromolecules along the yarn's main axis (fig. S7A), with the percentage of aligned yarns increasing from 66.1% at no-stretch to

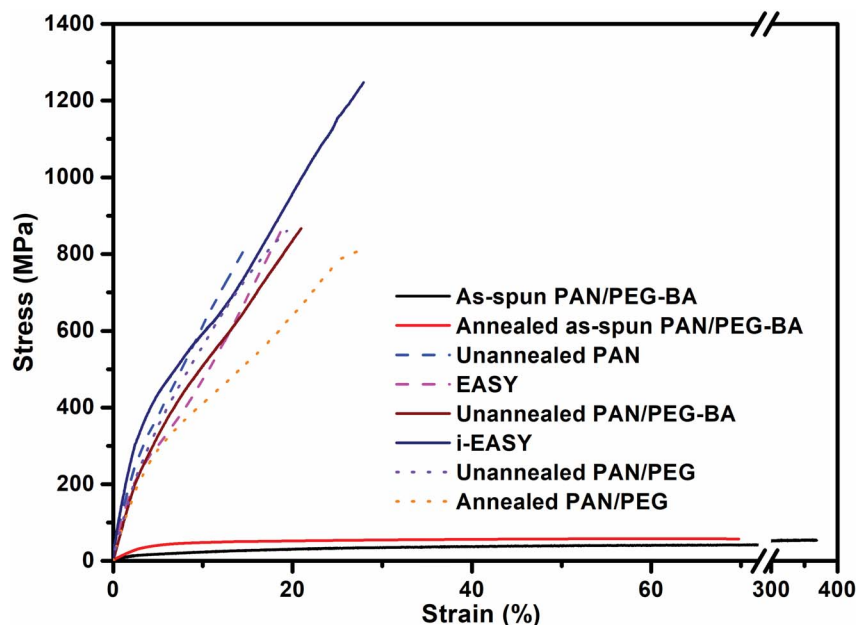


Fig. 2. Comparison of different yarns. Stress-versus-strain curves of unannealed and annealed (130°C for 4 hours) yarns (at SR 8) with 0 wt % PEG-BA, 4 wt % PEG-BA, and 4 wt % PEG.

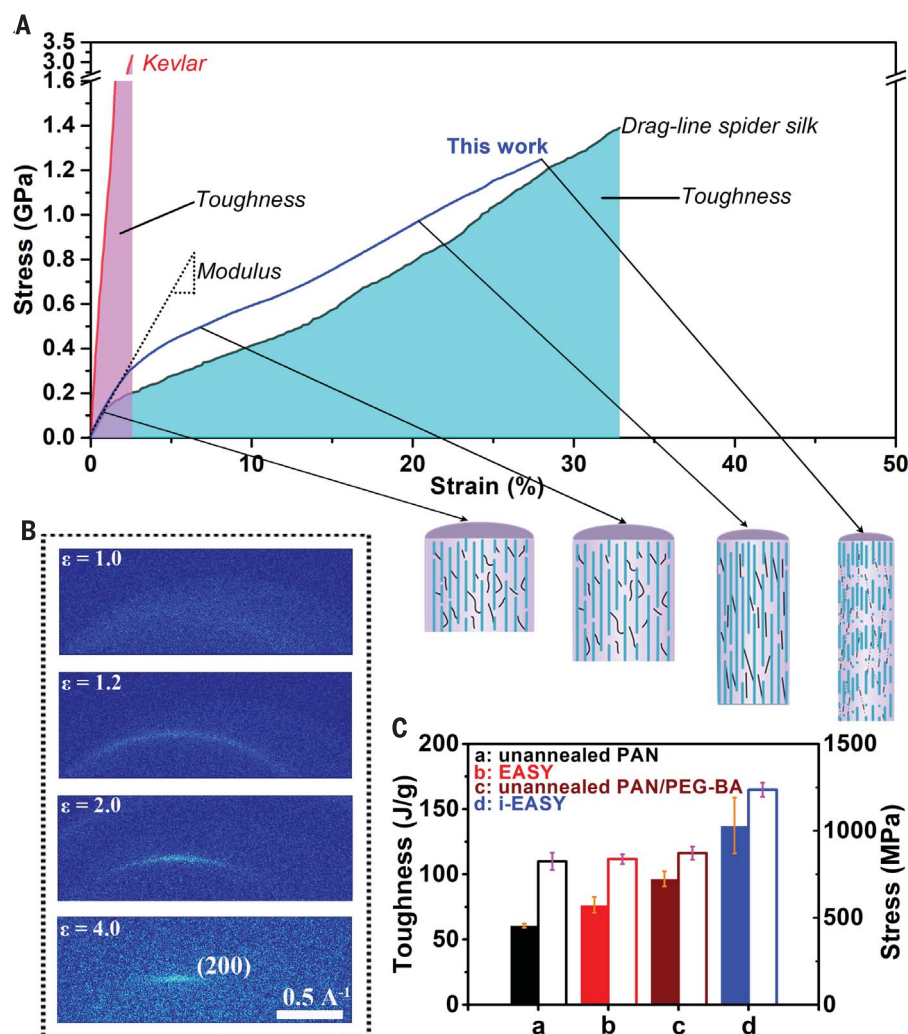


Fig. 3. Comparison of tensile strength and toughness of stretched and annealed yarns and their crystallization during heat stretching. (A) Comparison of stress-strain behavior and toughness of yarns (at SR 8 at 160°C, annealed at 130°C for 4 hours) with dragline spider silk and Kevlar [silk and Kevlar data are taken from the literature (16, 25)]. A model for the stress/strain behavior of yarns is presented beneath the graph. The blue lines represent PAN fibrils, and the black lines denote PEG-BA moieties. (B) In situ 2D-WAXS patterns recorded during the stretching process of a single yarn at 160°C. With increasing extension, we observe the development of a sharp Debye-Scherrer ring, subsequently followed by the development of a sharp (200) reflection, indicating crystal formation and alignment with high-orientation orders. (C) Comparison of the toughness (filled columns) and strength at break (open columns) of unannealed and annealed yarns with a SR 8 at 160°C. Error bars indicate the standard deviation of toughness and strength.

83.3% at SR 8 (stretched at 160°C). Wide-angle x-ray scattering experiments demonstrated that heat stretching resulted in a marked increase in the crystallinity from ~56.9% (at no stretch) to ~92.4% (at SR 9; fig. S7B), whereas annealing alone did not significantly increase crystallinity (fig. S7C). The size of the crystallites increased during stretching, from ~3.4 nm (as-spun) to ~12.9 nm and accompanied the increase in the degree of crystallinity (at SR 9; fig. S7D). Tensional forces during annealing are necessary to preserve the high degree of crystalline orientation. This is also supported by in situ x-ray

diffraction measurements of the crystalline orientation during stretching at 160°C (Fig. 3B). The crystallinity orientational order parameter (22) increased from 0.37 to 0.96 by heat stretching, but no significant increase was observed upon annealing (Fig. 3B and fig. S7, E to I). If no tension force was applied, the orientation parameters dropped from 0.96 to 0.82 during annealing because of thermal motion, which caused macromolecular relaxation and a reduction in the mechanical properties.

We analyzed the development of the specific strength and toughness throughout different

steps of preparation, which are: as-spun (green star in fig. S8), stretched (purple star in fig. S8), and finally annealed (blue oval in fig. S8). The strength primarily increased because of the stretching, whereas the toughness increased because of the annealing after stretching, which caused alignment of the fibrils and crystallization of PAN.

Too much PEG-BA can have an adverse impact on fibril resilience. Yarns with 5 wt % and 6 wt % PEG-BA featured lower strength and toughness than those with 4 wt % PEG-BA (fig. S5, E and F). Simultaneously, control experiments were performed by obtaining yarns with PAN and pure PEG ($M_n = 1000$, 4 wt %) (Fig. 2), which show a slight decrease in tensile strength (from 858 ± 103 MPa to 784 ± 77 MPa) and modulus (from 7.6 ± 1.0 GPa to 7.3 ± 1.1 GPa), a big increase in elongation at break (from 18.0 ± 1.6 % to 27 ± 2.5 %), and a slight increase in toughness (from 83 ± 12.2 J/g to 89 ± 15.0 J/g) after annealing. The yarns consisting of PAN and PEG (4 wt % but without azide groups) have almost the same elongation at break as yarns made from PAN and PEG-BA (4 wt % with azide groups), but they have lower strength. This suggests that the flexible oligomer PEG makes the yarns have higher elongation at break but lower strength than the PEG-BA yarns, due to the missing interaction between the fibrils. The interaction between cyano groups and PEG in the presence of azide groups was confirmed by $^1\text{H-NMR}$, $^{13}\text{C-NMR}$ (carbon-13 nuclear magnetic resonance), and ATR-FTIR (attenuated total reflectance–Fourier transform infrared spectroscopy) spectra (figs. S9 to S12). A new peak at about 4.2 parts per million (ppm) in $^1\text{H-NMR}$ and 162 ppm in $^{13}\text{C-NMR}$ spectra represents the carbon in the tetrazole after reaction between nitrile and azide groups. Further, a decreased intensity of the peak at 2100 cm^{-1} represents azide groups in the ATR-FTIR spectra, which suggests that the nitrile group in the PAN and azide groups in the PEG-BA can have a reaction in the yarns during the annealing process. i-EASYs are still soluble in N,N' -dimethylformamide and do not show any increase in molecular weight according to gel permeation chromatographic analysis, which strongly supports the idea that intermolecular cross-linking reactions of PAN molecules in the bulk of the fibrils did not occur. The most plausible explanation for these findings is that the reaction occurs only on the surface of the fibrils. Therefore, we postulate that under the presented conditions, interfibrillar reactions via PEG-BA are the dominating reaction.

A possible model for understanding the mechanical properties of i-EASY is shown in Fig. 3A. It highlights a reduction in the fractional-free volume after strain-induced crystallization and shrinking. As a result, PEG-BA macromolecules in the PAN matrix probably diffuse

to the fibril-free surface, which is the optimal position for efficient interfibrils reaction. Too much PEG-BA may lead to PEG microphases that represent defect structures that deteriorate the mechanical properties. Starting from pristine yarns, the PAN fibrils in the yarns begin to disentangle, resulting in a yield point. Beyond the yield point, the PEG-BA moieties bridging the PAN fibrils are responsible for stress transfer, impeding their ability to slide along and over each other. At a critical stress, the PEG-BA bridges might rupture, causing the yarns to break. This mechanism can be illustrated assuming the case of a single craze propagating ahead of the crack during stable crack growth. Then the local crack driving force (23, 24) is $\sim \frac{1}{\sqrt{E_1 E_2}}$, where, E_1 is the modulus in the fibril direction and E_2 is the modulus perpendicular to the fibrillar direction, which can be related to the PEG-BA elastic modulus. Thus, increasing E_2 should result in delaying the crack propagation. This mechanism is also supported by the fact that, at higher cross-linking density, the mechanical properties worsen.

To achieve the high strength and high toughness combination, annealing was required in addition to orientation and crystallization. Though single-polymer nanofibers could yield very high strength and high toughness, the handling difficulty of these single nanofibers has prevented their use in real-world applications. The presented process yields ultrafine electrospun yarns robust enough for practical use,

through a combination of thousands of fibrils with high alignment and interfibrillar reactions. We are convinced that ultrafine polymer yarns, as we show here, are not restricted to the present system. An important precondition for other systems is the extensibility of the yarn for orientation of the fibrils and reactive groups for interlinking of the fibrils.

REFERENCES AND NOTES

1. R. O. Ritchie, *Nat. Mater.* **10**, 817–822 (2011).
2. M. F. Ashby, *Materials Selection in Mechanical Design*, (Butterworth & Heinemann, ed. 2, 1999).
3. D. C. Hofmann *et al.*, *Nature* **451**, 1085–1089 (2008).
4. H. Zhu *et al.*, *Proc. Natl. Acad. Sci. U.S.A.* **112**, 8971–8976 (2015).
5. M. D. Demetriou *et al.*, *Nat. Mater.* **10**, 123–128 (2011).
6. A. B. Dalton *et al.*, *Nature* **423**, 703 (2003).
7. M. Naraghi *et al.*, *ACS Nano* **4**, 6463–6476 (2010).
8. Z. Xu *et al.*, *Adv. Mater.* **28**, 6449–6456 (2016).
9. J. Cai, M. Naraghi, *Carbon* **137**, 242–251 (2018).
10. A. Arinstein, M. Burman, O. Gendelman, E. Zussman, *Nat. Nanotechnol.* **2**, 59–62 (2007).
11. D. Papkov *et al.*, *ACS Nano* **7**, 3324–3331 (2013).
12. Y. Ding, H. Hou, Y. Zhao, Z. Zhu, H. Fong, *Prog. Polym. Sci.* **61**, 67–103 (2016).
13. J. H. Park, G. C. Rutledge, *J. Mater. Sci.* **53**, 3049–3063 (2018).
14. D. Papkov *et al.*, *ACS Nano* **13**, 4893–4927 (2019).
15. D. A. Tirrell, *Science* **271**, 39–40 (1996).
16. F. Vollrath, D. P. Knight, *Nature* **410**, 541–548 (2001).
17. K. Spiess, A. Lammel, T. Scheibel, *Macromol. Biosci.* **10**, 998–1007 (2010).
18. Z. P. Demko, K. B. Sharpless, *Angew. Chem. Int. Ed.* **41**, 2113–2116 (2002).
19. N. Yusof, A. F. Ismail, *J. Anal. Appl. Pyrolysis* **93**, 1–13 (2012).
20. For details of calculation, see supplementary materials.
21. T. Shen, C. Li, B. Haley, S. Desai, A. Strachan, *Polymer* **155**, 13–26 (2018).
22. Q. Ouyang *et al.*, *J. Macromol. Sci. B* **50**, 2417–2427 (2011).

23. H. R. Brown, *Macromolecules* **24**, 2752–2756 (1991).
24. H. H. Kausch, C. J. G. Plummer, *Polymer (Guildf.)* **35**, 3848–3857 (1994).
25. D. Zhu, X. Zhang, Y. Ou, M. Huang, *J. Compos. Mater.* **51**, 2449–2465 (2016).

ACKNOWLEDGMENTS

We thank R. Schneider for the GPC measurements, H. Schmalz and L. Benker for measurements of polarized Raman spectroscopy, P. Schmidt and T. Braun for support in construction of the yarn electrospinning set-up, S. Jiang for advice in electrospinning, and A. Wambach for technical support with figures and data arrangement. We acknowledge the use of the research facilities of the University of Bayreuth, the Bavarian Polymer Institute, the Institute of Physics - Martin-Luther-Universität Halle-Wittenberg, and the Forschungszentrum Jülich for this project. **Funding:** The work was supported by the University of Bayreuth (A.G.) and the Deutsche Forschungsgemeinschaft (WE4051/21-1 and 4051/22-1, to J.M.d.S.e.S.). **Author contributions:** A.G., X.L., and S.A. conceived and supervised the project. X.L. prepared the yarns; measured WAXS, TGA, NMR, and IR; and performed stress-strain tests. X.L., A.G., and S.A. wrote the manuscript. M.D. measured the crystal data and evaluated and discussed with S.F. X-ray computed tomography was performed by J.M.d.S.e.S. and was evaluated and discussed by J.M.d.S.e.S. and R.B.W. P.S. and H.H. evaluated and discussed the mechanical data of the yarns with X.L. and A.G. All authors contributed to the analysis and discussion of the data. The manuscript writing was led by A.G. with contributions from all other authors. **Competing interests:** The authors declare no competing interests. **Data and materials availability:** All data are available in the main text or the supplementary materials. Primary data are available from <https://myfiles.uni-bayreuth.de/ssf/s/readFile/share/31206/3130562511270201132/publicLink/Raw%20data%2020191018.zip>.

SUPPLEMENTARY MATERIALS

science.sciencemag.org/content/366/6471/1376/suppl/DC1
Materials and Methods
Figs. S1 to S12
Table S1
References (26–46)
Movies S1 to S4

27 July 2019; accepted 13 November 2019
10.1126/science.aay9033